Supporting information for

Reversible Zn-driven Reduction Displacement Reaction in Aqueous Zinc-ion Batteries

Lutong Shan,[a] Jiang Zhou*, [a] Mingming Han, [a] Guozhao Fang, [a] Xinxin Cao, [a] Xianwen Wu*,[b] and Shuquan Liang *,[a]

a School of Materials Science and Engineering, Central South University, Changsha 410083, P. R. China. E-mail: zhou_jiang@csu.edu.cn, lsq@csu.edu.cn

b School of Chemistry and Chemical Engineering, Jishou University, Jishou 416000, P.R. China. E-mail: wxwcsu2011@163.com

1. Experimental

Synthesis. All the reactants were used as-received without further purification. Typically, 0.3 g of V_2O_5 was mixed with 30 mL deionized water with 4 mL H_2O_2 added dropwise. After stirred at 40℃ for 30 min, 398.27 mg of $Cu(NO_3)_2 \cdot 3H_2O$ was added to the above orange solution with further 30 min stirring at 40℃. Then the mixed solution was transferred into 50 mL Teflon-lined autoclave and heated at 200 ℃ for 48 h. Finally, the $Cu_3(OH)_2V_2O_7 \cdot 2H_2O$ nanosheet were obtained after centrifuged several times with alcohol and dried overnight.

Material Characterization. In our research, the X-ray power diffraction (XRD) are applied to determine the phase of the as-prepared $Cu_3(OH)_2V_2O_7 \cdot 2H_2O$. And Scanning electron microscopy (SEM, FEI Nova NanoSEM 230m, 10 kV) and transmission electron microscopy (TEM, Titan G2 60-300) are applied to acquire the microcosmic crystal morphologies and sizes. X-ray photoelectron spectroscopy (XPS) spectra were performed on an ESCALAB 250Xi X-ray photoelectron spectrometer (Thermo Fisher).

Electrochemical Measurements. In the typical synthesis, the as-prepared $Cu_3(OH)_2V_2O_7 \cdot 2H_2O$ material were mixed with acetylene black and polyvinylidene fluoride in N-methy-2-pyrrolidone (NMP) in the weight ratio of 70:20:10 to make a slurry, which latter was used to coat the thin stainlesssteel mesh and then dried in a vacuum oven at 80℃ for 12h. Then the coin cell assembly was executed in air condition, with the zinc metal as the anode and 3M solution of $ZnSO_4$ as the electrolyte. The measurements of the specific capacity and rate capability was performed in Land Battery Tester (Land CT 2001A) within the voltage window of 0.4-1.4V (versus Zn/Zn^{2+}). Besides, electrochemical workstation (MULTI AUTOLAB M204, Metrohm) was used to measure the cyclic voltammetry (CV) curves at a scan rate of 0.1

mV s^{-1} during the voltage scale of 0.4-1.4 V (versus Zn/Zn^{2+}) and the electrochemical impedance spectrometry (EIS) from 100 kHz to 10 mHz. Arbin instruments (S/N 170539) was applied to measure the GITT results. The loading of composites for each electrode in this experiment is about 1.2-1.6 mg with an area of 1.1304 cm^2.

2.

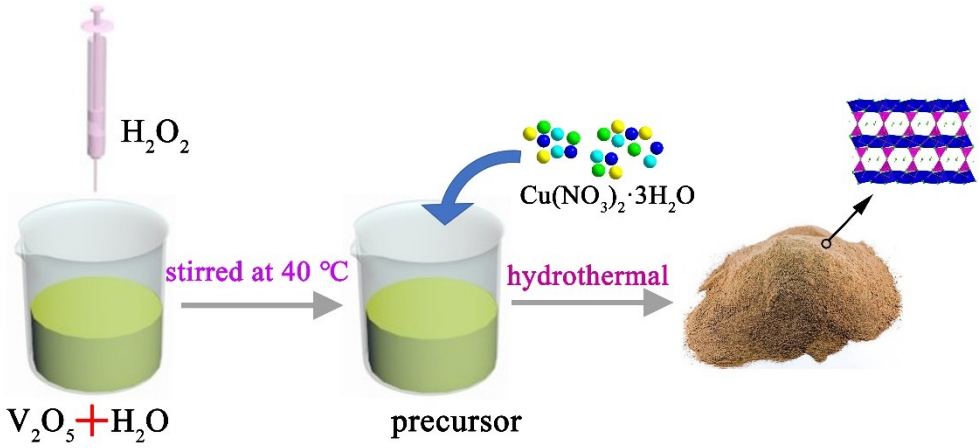

Figure S1 Illustration of the synthesis process of $Cu_3(OH)_2V_2O_7{\cdot}2H_2O$ nanosheet.

3.

Figure S2 The successful light up of LED lamp bank with four aqueous Zn/$Cu_3(OH)_2V_2O_7 \cdot 2H_2O$ coin-cells.

4.

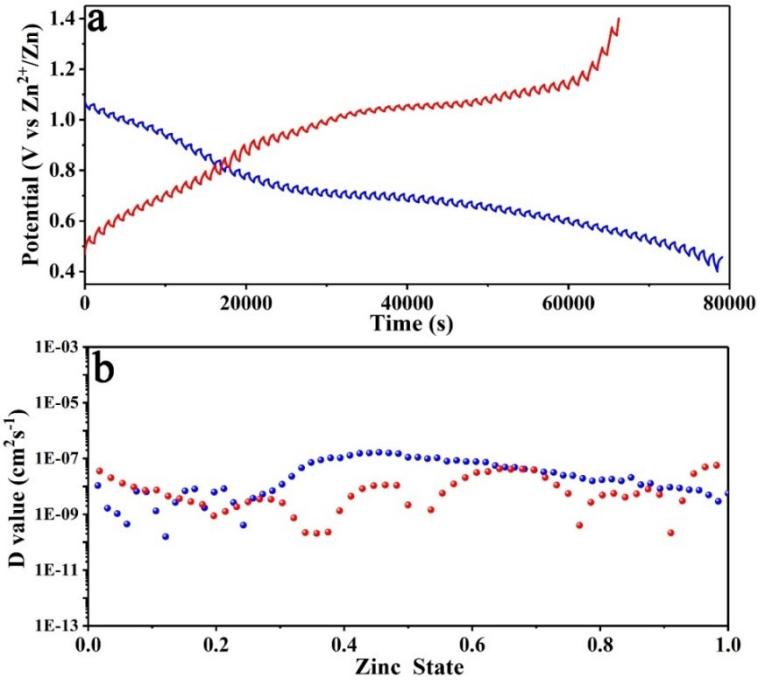

Figure S3 (a) The discharge-charge GITT curves and (b) the zinc ion diffusion coefficient of $Cu_3(OH)_2V_2O_7{\cdot}2H_2O$ material.

The diffusion coefficient of Zn^{2+} could be measured by using Ganlvanostatic Intermittent Titration Technique (GITT) technique and calculated via the following equation[1-4]:

$$D = \frac{4L^2}{\pi\tau}\left(\frac{\Delta E_S}{\Delta E_t}\right)^2$$

In the above equation, t and τ represent the duration of current pulse (s) and relaxation time (s), respectively. L corresponds to Zn^{2+} diffusion length, which is equal to thickness of electrode. ΔE_S and ΔE_t are the steady-state voltage change (V) by the current pulse and voltage change (V) during the constant current pulse (eliminating the voltage changes after relaxation time).

5.

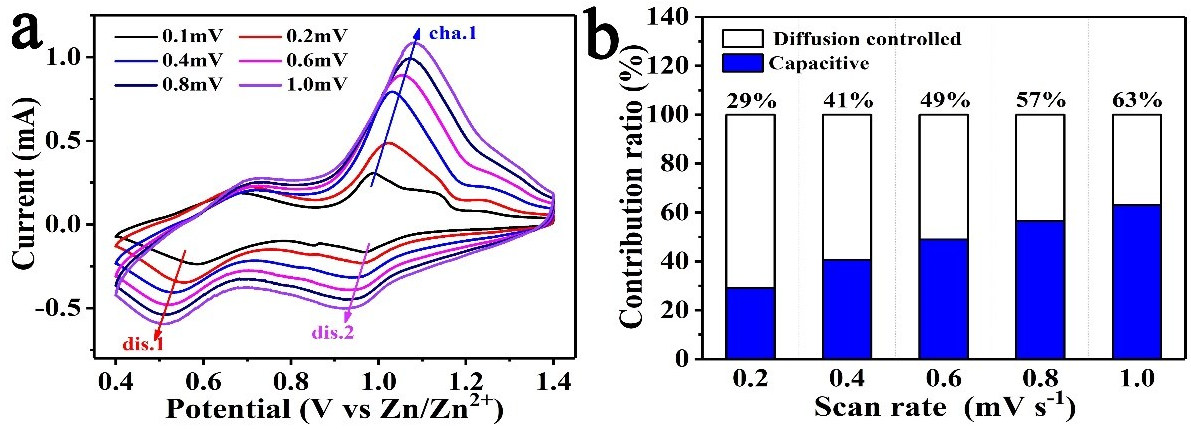

Figure S4 (a) CV curves at various scan rates of 0.1-1.0 mV s^{-1}, (b) Contribution ratios comparison of capacitive effect and diffusion process at various scan rates.

As elucidated,[5] the kinetic of capacitive contribution can be obtained through calculating the CV curves at different scan rates. It is ought to be noted that there is a power law that links the scan rate with the current, which is: $i=av^b$. Here, the equation can be converted as: $log(i)=log(a)+b*log(v)$, henceforth, by calculating the value of log(i) and log(v), we can reach a precise *b* value via a consequent mathematical fitting. As known, if the value of *b* is 0.5, we can summarize that the capacity is fully contributed by diffusion process, while the *b* value is 1, we can conclude that the capacity is ruled by the capacitive effect.

Furthermore, there is an equation that matches the two factors of diffusion-controlled contribution and the capacitive effects with the current, which is: $i=k_1v^{1/2}+k_2v$.

In this formula, when the k_1 value reaches for 0, then it turns to be: $i= k_2v$, which is similar to $i=av$, and we can reasonably speculate that the capacity is mainly ascribed to capacitive effect. The same way, when the k_2 value is close to 0.5, which makes the equation agree well with $i=av^{0.5}$, then it can be deduced that diffusion-controlled process mostly account for

capacity, typically. As shown in **Fig. S4b**, with the increasing scan rates, the capacitive contribution ratio emerges an increasing trend.

6.

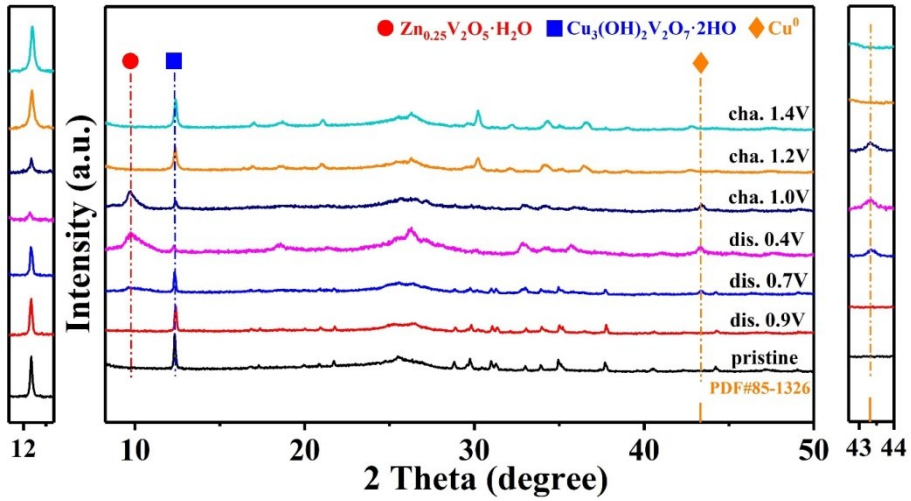

Figure S5 *Ex-situ* XRD measurements at different discharge-charge states of $Cu_3(OH)_2V_2O_7{\cdot}2H_2O$ material with carbon cloth as current collector.

7.

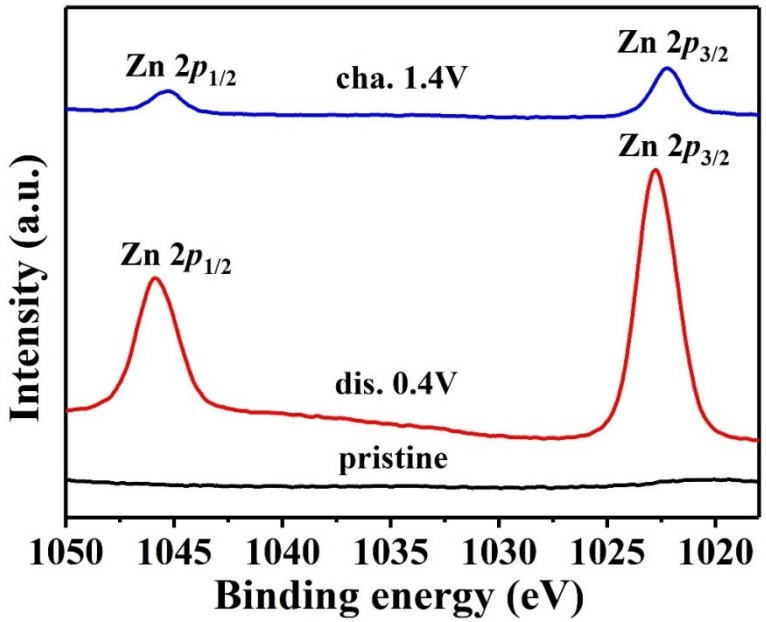

Figure S6 The Zn 2*p* spectra at various states of pristine, completely discharged and completely charged.

8.

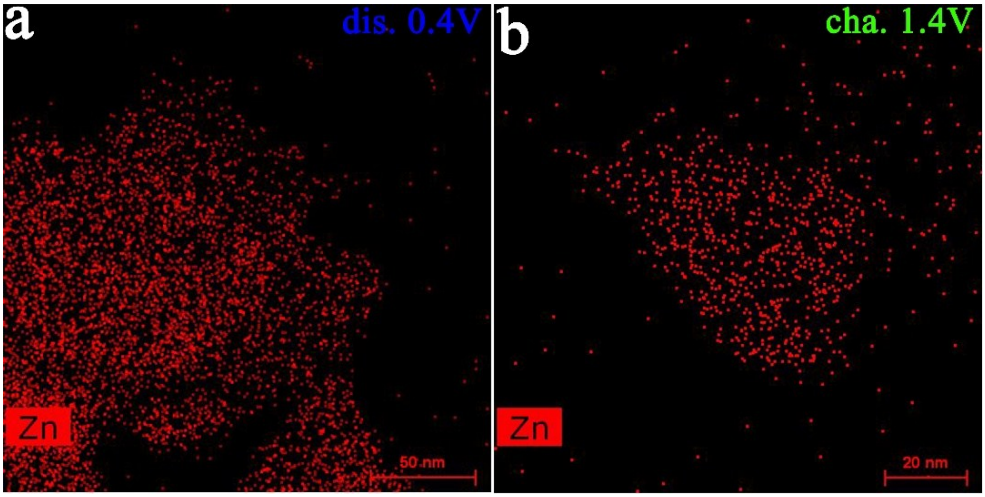

Figure S7 Zn^{2+} ions EDS element mapping of $Cu_3(OH)_2V_2O_7 \cdot 2H_2O$ product at (a) fully discharged and (b) fully charged state.

9.

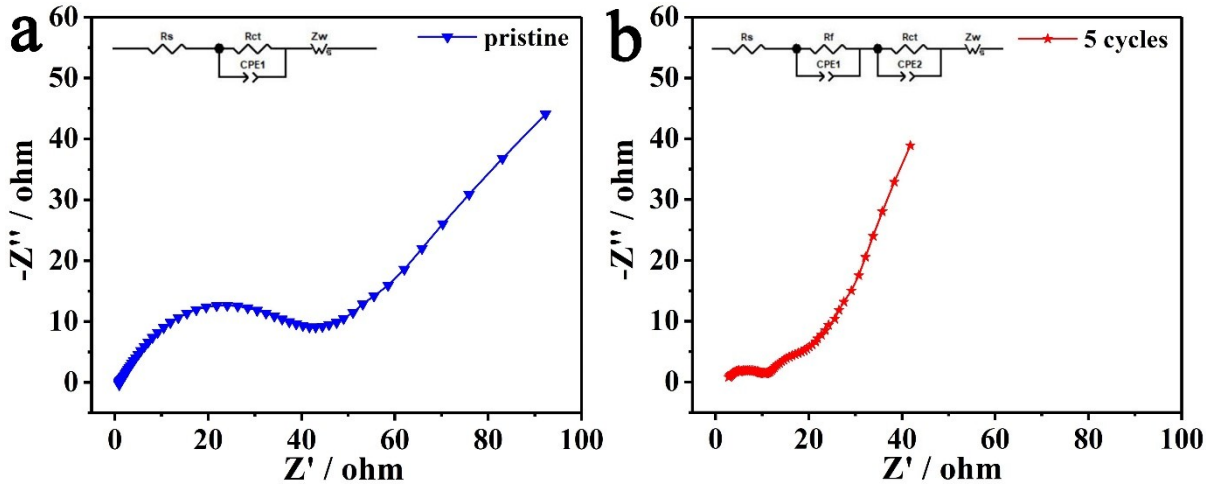

Figure S8 The EIS results and correspond equivalent electrical circuits of $Cu_3(OH)_2V_2O_7{\cdot}2H_2O$ cathode at (a) pristine state and (b) after 5 cycles.

$\boldsymbol{R_s}$ represents the electrolyte resistance, $\boldsymbol{R_f}$ suggests the resistance of SEI layer and $\boldsymbol{R_{ct}}$ represents the charge-transfer resistance. In **Fig. S8**, the EIS results and correspond equivalent electrical circuits indicate that SEI layer does not exist at pristine state and appears after 5 galvanostatic discharge-charge cycles, contributing to the resistance ($\boldsymbol{R_f}$). The primary EIS simulation parameters can be seen in **Table S1**. After 5 cycles, $\boldsymbol{R_s}$ remains stable, and $\boldsymbol{R_{ct}}$ manifests significant decrease from 41.02 Ω to 20.83 Ω, which could be attributed to the formation of metallic Cu^0 upon discharge as well as the activation process.[6, 7]

10.

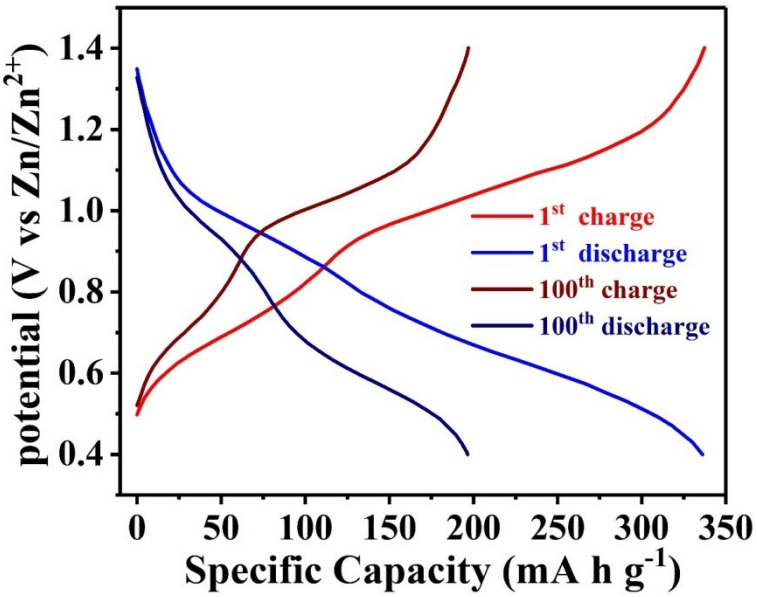

Figure S9 The discharge-charge profiles at 1st and 100th cycle of $Cu_3(OH)_2V_2O_7 \cdot 2H_2O$ at 1 A g^{-1}.

11. Table S1 The Primary EIS Simulation Parameters of $Cu_3(OH)_2V_2O_7 \cdot 2H_2O$ electrodes

Samples	R_s (Ω)	R_f (Ω)	R_{ct} (Ω)
pristine	**6.178**	**-**	**41.02**
5 cycles	**5.714**	**3.252**	**20.83**

Reference

1. A. K. Jordan Anderson, Diego J. Dı´az and Sudipta Seal, *J. Phys. Chem. C*, 2010, **114**, 4595–4602.
2. B. A. B. a. R. A. H. C. JohnWen, *J. Electrochem. Soc.*, 1979, **126**, 2258-2266.
3. W. W. a. R. A. Huggins, *J. Electrochem. Soc.*, 1977, **124**, 1569-1577.
4. D. T. Ngo, H. T. T. Le, C. Kim, J.-Y. Lee, J. G. Fisher, I.-D. Kim and C.-J. Park, *Energy Environ. Sci.*, 2015, **8**, 3577-3588.
5. W. Wen, J.-M. Wu, Y.-Z. Jiang, L.-L. Lai and J. Song, *Chem*, 2017, **2**, 404-416.
6. W. Ren, H. Zhang, C. Guan and C. Cheng, *Adv. Funct. Mater.*, 2017, **27**, 1702116.
7. J. Xu, M. Wang, N. P. Wickramaratne, M. Jaroniec, S. Dou and L. Dai, *Adv. Mater.*, 2015, **27**, 2042-2048.